Visualization of Pit-1 Transcription Factor Interactions in the Living Cell Nucleus by Fluorescence Resonance Energy Transfer Microscopy

Richard N. Day

Departments of Medicine and Cell Biology
National Science Foundation Center for Biological Timing
University of Virginia Health Sciences Center
Charlottesville, Virginia 22908

The pituitary-specific transcription factor Pit-1 forms dimers when interacting with specific DNA elements and has been shown to associate with several other nuclear proteins. Recently, techniques have become available that allow visualization of protein-protein interactions as they occur in single living cells. In this study, the technique of fluorescence resonance energy transfer (FRET) microscopy was used to visualize the physical interactions of Pit-1 proteins fused to spectral variants of the jellyfish green fluorescent protein (GFP) that emit green or blue light [blue fluorescent protein (BFP)]. An optimized imaging system was used to discriminate fluorescence signals from single cells coexpressing the BFP- and GFP-fusion proteins, and the contribution of spectral overlap to background fluorescence detected in the FRET images was established. Energy transfer signals from living cells expressing a fusion protein in which GFP was tethered to BFP by short protein linker was used to demonstrate acquisition of FRET signals. Genetic vectors encoding GFP- and BFP-Pit-1 proteins were prepared, and biological function of the fusion proteins was confirmed. FRET microscopy of HeLa cells coexpressing the GFP- and BFP-Pit-1 demonstrated energy transfer, which required the two fluorophores to be separated by less than 100 Å. Biochemical studies previously demonstrated that Pit-1 physically interacts with both c-Ets-1 and the estrogen receptor. FRET imaging of cells coexpressing BFP-Pit-1 and GFP-Ets-1 demonstrated energy transfer between these fusion proteins, a result consistent with their association in the nucleus of these living cells. In contrast, there was no evidence for energy transfer between the BFP-Pit-1 and an estrogen receptor-GFP fusion proteins. It is likely that the FRET imaging approach described here can be applied to many different protein-partner pairs in a variety of cellular contexts. (Molecular Endocrinology 12: 1410–1419, 1998)

0888-8809/98/$3 00/0
Molecular Endocrinology

INTRODUCTION

Determining when and where specific protein partners associate with one another within the cell is of fundamental importance to understanding biological processes. The relative proximity of two proteins labeled with different fluorophores can be determined by conventional fluorescence microscopy to the scale of approximately 0.2 μm (2000 Å), the limit of optical resolution for the light microscope. Resolving the relative proximities of proteins beyond the optical limit of the microscope, however, is necessary to reveal the physical interactions between protein partners. For the light microscope, this degree of resolution can only be realized through the use of fluorescence resonance energy transfer (FRET; Refs. 1–4). FRET is a quantum mechanical process by which radiationless transfer of excitation energy can occur from a donor fluorophore to an appropriate acceptor fluorophore. Energy transfer requires that the donor fluorophore emission spectrum overlap with the absorption spectrum for the acceptor fluorophore. Because the efficiency of energy transfer varies inversely with the sixth power of the distance separating the two fluorophores, FRET can only occur when the distance separating the two fluorophores is less than approximately 0.01 μm (100 Å; Refs. 1–4). Thus, FRET microscopy is an extraordinarily sensitive method for determining the relative proximity of labeled protein partners.

A major obstacle to the application of FRET microscopy to living cells has been a lack of suitable methods for specifically labeling intracellular proteins with donor and acceptor fluorophores. Recent studies using expression of the jellyfish green fluorescent protein

(GFP) in a variety of cell types have proven this unique protein to be a versatile molecular reporter (5–9). GFP retains its characteristic fluorescence when fused to other protein sequences, allowing fluorescence microscopy to be used to visualize the spatiotemporal dynamics of GFP-fusion protein localization in intact living cells (9–12). Mutant forms of GFP with emission in both the green and the blue spectrum [blue fluorescent protein (BFP)] have been engineered (5, 6, 8). These different color fluorophores provide a general method for simultaneously labeling two different proteins within the same living cell (9). Importantly, the excitation and emission spectra for the mutant GFP and BFP proteins are suitable for FRET, making this unique noninvasive imaging approach more generally applicable (8, 13–17).

We reported previously the optimization of a fluorescence microscope imaging system for the acquisition of green, blue, and energy transfer fluorescence signals from single living cells expressing GFP- and BFP-fusion proteins (15–17). In the present study, the FRET approach is applied to visualize protein-protein interactions involving the pituitary-specific transcription factor Pit-1. The Pit-1 protein dimerizes when associated with specific DNA elements of target genes. Moreover, cooperative interactions between Pit-1 and other classes of transcription factors were shown to be important for hormone and growth factor regulation of Pit-1-dependent gene expression. For example a strong synergy between Pit-1 and members of the *ets* transcription factor family was shown to be involved in regulation of PRL gene transcription (18, 19), and biochemical studies showed a physical association of Pit-1 and Ets-1 (20). In addition, cooperative interactions between the Pit-1 protein and the estrogen receptor were also shown to be important in regulation of the PRL gene transcription (21, 22), and a physical association of these two proteins was demonstrated (23, 24). The studies presented here use GFP- and BFP-fusion proteins and the FRET technique to visualize homologous interactions involving the Pit-1 protein and heterologous interactions between Pit-1 and the Ets-1 or estrogen receptor proteins in the living cell nucleus.

RESULTS

The GFP-Fusion Proteins Are Biologically Functional

Genetic vectors encoding GFP- and BFP-fusion proteins were used in transient cotransfection of HeLa cells to achieve cellular expression of the protein partners. In each case, expression of the fusion proteins was confirmed by Western blotting (see individual figures). The expression vectors for GFP-Pit-1 and BFP Pit-1 encoded proteins with the fluorophores tethered to the amino-terminal end of Pit-1 by a five-amino acid (AA) linker (see *Materials and Methods* and Ref. 15). Several different methods were used to demonstrate that these fusion proteins were functional. First, Western blotting was used to demonstrate that the expected 60-kDa GFP-Pit-1 was synthesized in transfected cells (*inset*, Fig. 1). Second, the GFP-Pit-1 protein was shown to bind to both the PRL gene 3P Pit-1 DNA element (*inset* Fig. 1) and 1P element (not shown) using the gel mobility shift assay (EMSA). The specificity of this DNA-protein complex was demonstrated by immunoclearing of the complex from the EMSA reaction by addition of an antibody specific for Pit-1 (*inset*, Fig. 1). Further, competition studies with

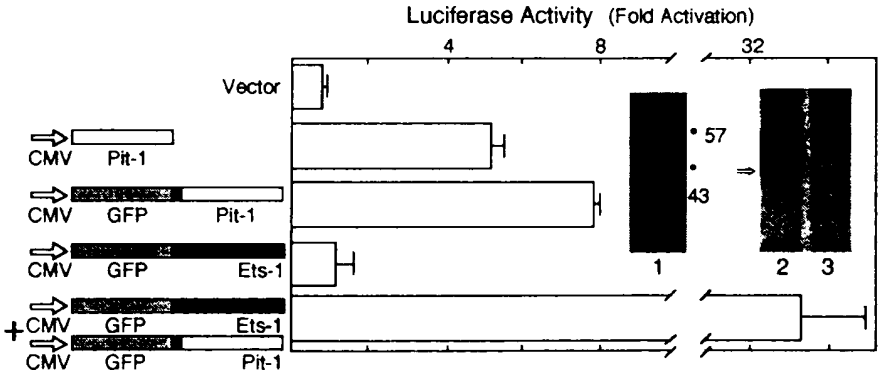

Fig. 1. GFP-Pit-1 and GFP-Ets-1 Fusion Proteins Are Biologically Functional

Representative experiment demonstrating transcriptional activation of the −306 rat PRL promoter luciferase reporter gene by cotransfection with CMV Pit-1 or CMV GFP-Pit-1 expression vectors. Much greater than additive luciferase activity was observed when CMV GFP-Pit-1 and CMV GFP-Ets-1 were cotransfected than when they are transfected separately (note scale break). Results are triplicate transfections plotted as fold activation over the empty vector control ± SE. *Inset*, Western blot analysis of GFP-Pit-1 protein in extracts from transiently transfected cells probed with an antibody directed against GFP (lane 1). *Numbers* indicate size marker migration EMSA demonstrating binding of proteins from whole-cell extracts prepared from Rat-1 cells transfected with the CMV GFP-Pit-1 plasmid to a duplex ^{32}P-labeled 3P PRL Pit-1 site probe (lane 2). DNA-protein complex (*arrowhead*) was not observed for extracts pretreated with a polyclonal antibody directed against Pit-1 (lane 3).

unlabeled oligonucleotides confirmed the fusion protein-bound DNA with appropriate binding specificity, and the fusion protein did not bind to an unrelated interferon response element (data not shown). Importantly, the results shown in Fig. 1 demonstrated that expression of GFP-Pit-1 induced transcription from a cotransfected PRL promoter-luciferase reporter gene to a similar extent as the wild-type Pit-1 protein. Moreover, the GFP-Pit-1 protein was also shown to synergize with a GFP-Ets-1 protein in activation of the PRL gene promoter (Fig. 1). These results confirmed that the GFP-Pit-1 fusion protein retained the characteristics of specific DNA binding, transcriptional activation, and cooperative interactions with Ets-1.

Characterizing Spectral Overlap

FRET microscopy requires an imaging system that can discriminate fluorescence signals with overlapping spectra. We previously reported the use of GFP- and BFP-fusion proteins to characterize and optimize excitation and emission filters for detection of blue and green fluorescence signals from individual living cells (15–17). In the present study, the extent of blue-fluorescence overlap into the filter set used to detect energy transfer (the acceptor filter set) was quantified. This is important, since this signal overlap contributes to the background signal against which energy transfer signals will be compared. HeLa cells were transfected with the expression vector encoding BFP-Pit-1, and the expression of the expected 60-kDa protein was verified by Western blotting (Fig. 2A). Cells expressing the BFP-Pit-1 fusion protein were then identified by nuclear-localized blue fluorescence (Fig. 2C). Images of cells expressing BFP-Pit-1 were then obtained under constant conditions of neutral density (nd) and integration time with each of the three filter combinations used in these studies (Fig. 2, B–D; see *Materials and Methods* for filter characteristics). After background subtraction, a mosaic of the donor (BFP-Pit-1) and acceptor (overlap) images was generated and a look-up table was applied to the gray scale image to quantify signal intensity (Fig. 2, C and D; white indicates highest fluorescence signal). The gray level intensity of the donor and acceptor fluorescence signals across the profile of the nucleus was then determined for each image (position of the profiles is indicated by lines in Fig. 2, C and D), and the results were plotted (Fig. 2, E and F). The results shown in Fig. 2, E and F, quantify the intensity of the BFP fluorescence detected by both the donor and acceptor filter sets, demonstrating the extent of BFP-fluorescence signal overlap into the acceptor (FRET) image.

Since the FRET technique requires discrimination of green and blue fluorescence signals, imaging of cells expressing colocalized BFP- and GFP-fusion proteins that would not be expected to physically interact was used to characterize further the extent of fluorescence signal overlap detected with the acceptor filter set. HeLa cells were cotransfected with the vector encoding BFP-Pit-1 and a vector encoding GFP with a nuclear localization signal (GFP-NLS; see *Materials and Methods* for sequence). Western blotting was used to demonstrate that both the 29-kDa GFP-NLS and 60-kDa BFP-Pit-1 fusion proteins were expressed in transiently transfected cells (Fig. 3 A). As noted above, the BFP-Pit-1 protein was exclusively localized to the nucleus, and coexpression with the GFP-NLS resulted in both green and blue fluorophores in the nuclear compartment (Fig. 3, B and C). Background subtracted donor (BFP-Pit-1) and acceptor images were acquired under constant conditions of nd and image acquisition time, and the same look-up table was applied to the mosaic image to show fluorescence intensity (Fig. 3, C

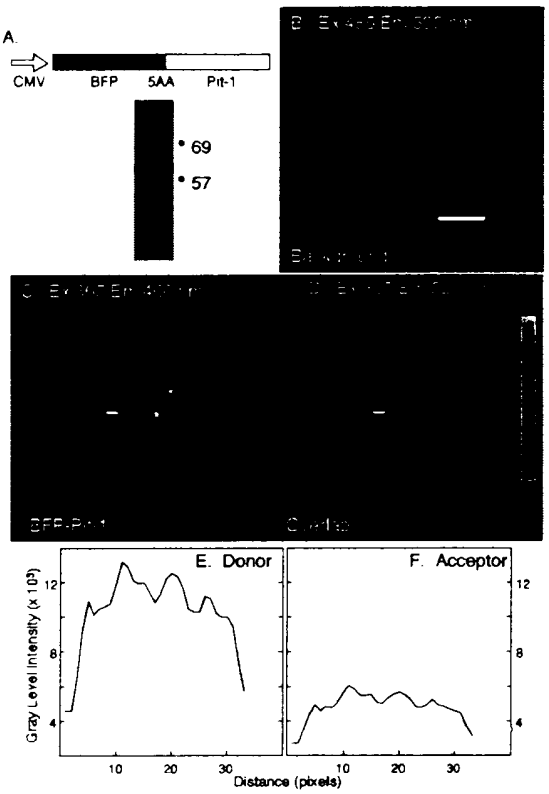

Fig. 2. Characterization of BFP Fluorescence Overlap in the Acceptor Image

HeLa cells were transiently transfected with the CMV BFP-Pit-1 vector and expression of the fusion protein was detected by Western blot (A). Images of a cell expressing the fusion protein were obtained using a nd 1.0 filter and 1-sec integration with the GFP filter set (panel B; bar indicates 10 μm), or 5-sec integration with the BFP filter set (C) and the acceptor filter set (D). The donor and acceptor images were combined in a single mosaic image (panels C and D), and a look-up table was applied to facilitate comparison of fluorescence signal intensity (*calibration bar* indicates signal level with *white* being highest intensity). A profile was taken across the cell nucleus at the position indicated by the lines in panels C and D, and the gray level intensity for this profile was plotted for both the donor and acceptor images (panels E and F).

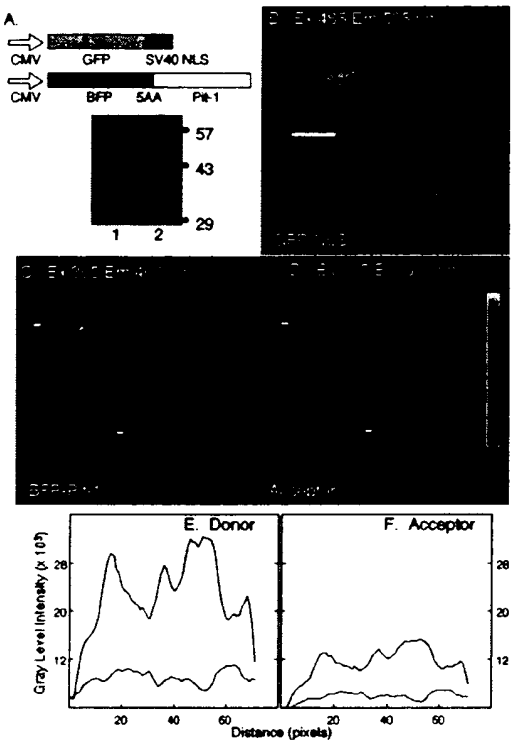

Fig. 3. Discrimination of Fluorescence Signals from Cells Expressing Noninteracting GFP- and BFP-Fusion Proteins

HeLa cells were transiently transfected with the CMV GFP-NLS or CMV BFP-Pit-1 vectors, and expression of the fusion proteins was detected by Western blot (panel A, lanes 1 and 2, respectively). Images of HeLa cells coexpressing these proteins were then obtained using the GFP filter set (panel B; *bar* indicates 10 μm), BFP filter set (C), and the acceptor filter set (D), and the mosaic image of donor and acceptor fluorescence (panels C and D) was acquired as described in the legend of Fig. 2. The gray level intensity profile across the nuclei of the two cells was taken at the position indicated by the lines in panels C and D and was plotted for both the donor and acceptor images (panels E and F).

and D). The gray level intensity for nuclear fluorescence at the indicated positions across the profile of the nuclei from these two cells was then determined. The results shown in Fig. 3, E and F, demonstrated the extent of combined GFP- and BFP-signal overlap detected with the acceptor filter set. For the cells shown in Fig. 3, the acceptor signal represents approximately 45% of the donor signal. Together, these results demonstrated the contribution of both GFP- and BFP-fusion protein fluorescence signal overlap into the acceptor image and established the baseline fluorescence against which FRET signals were compared.

Visualizing FRET from Single Living Cells

We and others demonstrated previously that energy transfer signals can be acquired from living cells expressing a fusion protein in which GFP is tethered directly to BFP through a protein linker (13–15, 17). This same approach was taken to characterize the acquisition of energy transfer signals under the constant conditions used in the present study. HeLa cells were transfected with an expression vector encoding GFP coupled to BFP through a three-AA linker and expression of the 56-kDa protein was confirmed by Western blotting (Fig. 4A). Cells expressing the fusion protein were identified by green fluorescence throughout the cell (Fig. 4B). Images of these cells were then acquired using the donor (BFP) and acceptor filter combinations, and the same look-up table was applied to the background-subtracted mosaic image to show the fluorescence signal intensity (Fig. 4, B and C). The gray level intensity across the profile of the two cells shown in Fig. 4 was determined at the positions indicated. In contrast to the results from the previous experiment with colocalized, but noninteracting flu-

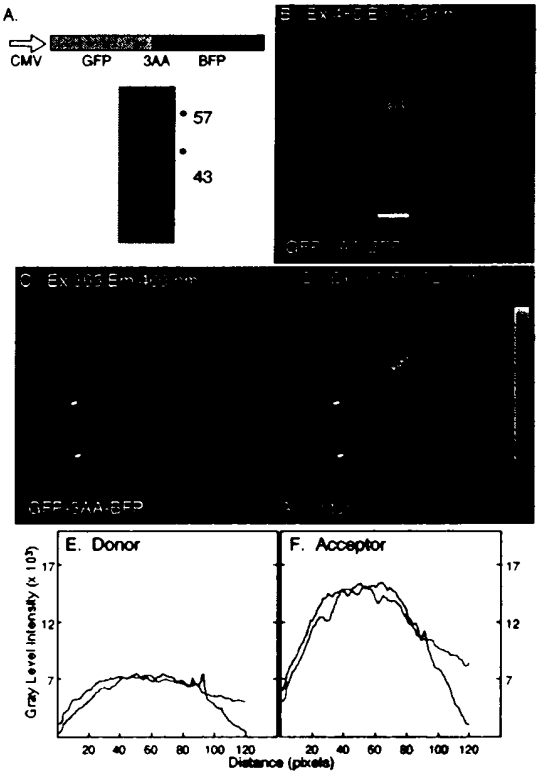

Fig. 4. FRET Microscopy of Cells Expressing GFP Fused Directly to BFP by a Three-AA Linker

HeLa cells were transiently transfected with the CMV GFP-three-AA-BFP vector, and expression of the protein was detected by Western blot (A). Images of two cells expressing the GFP-three-AA-BFP protein were obtained using the GFP filter set (panel B; *bar* indicates 10 μm), BFP filter set (C), and the acceptor filter set (D), and a mosaic image of donor and acceptor fluorescence (panels C and D) was acquired as described in the legend of Fig. 2. The gray level intensity profile across the two cells was taken at the position indicated in panels C and D and was plotted for both the donor and acceptor images (panels E and F).

orophores, the results shown in Fig. 4, E and F, demonstrated that the gray level intensity for the acceptor image was approximately 2-fold greater than the signal measured in the donor image. This result showed energy transfer from BFP to GFP.

Visualizing the Physical Association of Pit-1 Proteins

The FRET imaging approach described above was then applied to cells coexpressing the GFP- and BFP-Pit-1 fusion proteins. HeLa cells were cotransfected with vectors encoding the GFP-Pit-1 and BFP-Pit-1 fusion proteins, and expression of the fusion proteins was confirmed by Western blotting (Fig. 5A). Cells coexpressing the BFP-Pit-1 and GFP-Pit-1 proteins were first identified by green fluorescence (Fig. 5B).

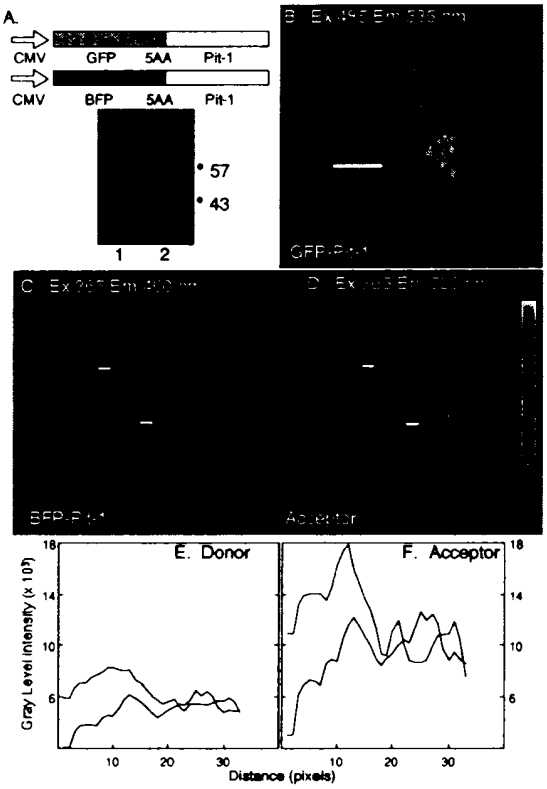

Fig. 5. FRET Microscopy of Cells Expressing GFP- and BFP-Pit-1 Proteins

HeLa cells were transfected with vectors encoding GFP-Pit-1 or BFP-Pit-1, and expression of the proteins was detected by Western blot (panel A, lanes 1 and 2, respectively). Images of HeLa cells cotransfected with these vectors were then obtained obtained using the GFP filter set (panel B; *bar* indicates 10 μm), BFP filter set (C), and the acceptor filter set (D), and a mosaic image of donor and acceptor fluorescence (panels C and D) was acquired as described in the legend of Fig. 2. The gray level intensity profile across the two cell nuclei were taken at the position indicated in panels C and D and was then plotted for both the donor and acceptor images (panels E and F).

Images of these same cells were then obtained under constant conditions of nd and integration time using the donor and acceptor filter sets. A mosaic image showing the background subtracted donor (BFP-Pit-1) and acceptor images was obtained, and the same look-up table was applied to indicate fluorescence intensity (Fig. 5, C and D). The gray level intensity across the profile of the two nuclei shown in Fig. 5 at the positions indicated was then plotted (Fig. 5, E and F). The results demonstrated that the acceptor signal exceeded the donor signal by approximately 2-fold, an indication of energy transfer from BFP-Pit-1 to GFP-Pit-1. This required that the fluorophores be separated by less than approximately 100 Å, as would be the case for physically associated Pit-1 fusion proteins.

FRET Imaging of Pit-1 and Ets-1 or the Estrogen Receptor

This imaging technique was then used to examine HeLa cells coexpressing the GFP-Ets-1 and BFP-Pit-1 fusion proteins. Cooperative interactions between the Pit-1 and Ets-1 proteins in the transcriptional activation of the PRL gene promoter were reported (18–20), and the GFP-Ets-1 protein used in the current study was shown to synergize with GFP-Pit-1 in transcriptional activation of a PRL promoter-luciferase reporter gene (Fig. 1). Western blotting of protein extracts from transiently transfected HeLa cells confirmed that both the 80- kDa GFP-Ets-1 and the 60-kDa BFP-Pit-1 fusion proteins were expressed (Fig. 6A). Cells expressing the GFP-Ets-1 protein were identified by green fluorescence, and coexpression of the BFP-Pit-1 protein was verified by presence of nuclear blue fluorescence (Fig. 6B). Images of cells coexpressing the two fusion proteins were then obtained under constant conditions of nd and integration time using the donor and acceptor filter sets. A mosaic image showing the background subtracted donor (BFP-Pit-1) and acceptor (GFP-Ets-1) images was obtained as described above (Fig. 6, C and D). The gray level intensity across the profile of the two nuclei shown in Fig. 6 at the positions indicated was then determined (Fig. 6, E and F). The results demonstrated that the fluorescence intensity in the acceptor image was greater than that for the donor image. The acceptor signal was above the base fluorescence established in the control experiments (Figs. 2 and 3), an indication that the Ets-1 and Pit-1 fusion proteins were in close association.

The FRET imaging approach was also applied to cells expressing Pit-1 and the estrogen receptor to determine whether a physical association between these two proteins could be detected. HeLa cells were cotransfected with an expression vector encoding the human estrogen receptor with GFP fused at the carboxy terminus [human estrogen receptor (hER)-GFP] and the BFP-Pit-1 fusion protein. Functional cooperativity between Pit-1 and the hER-GFP fusion protein was observed in cotransfection studies using a 3-kb rat PRL promoter/enhancer luciferase reporter gene

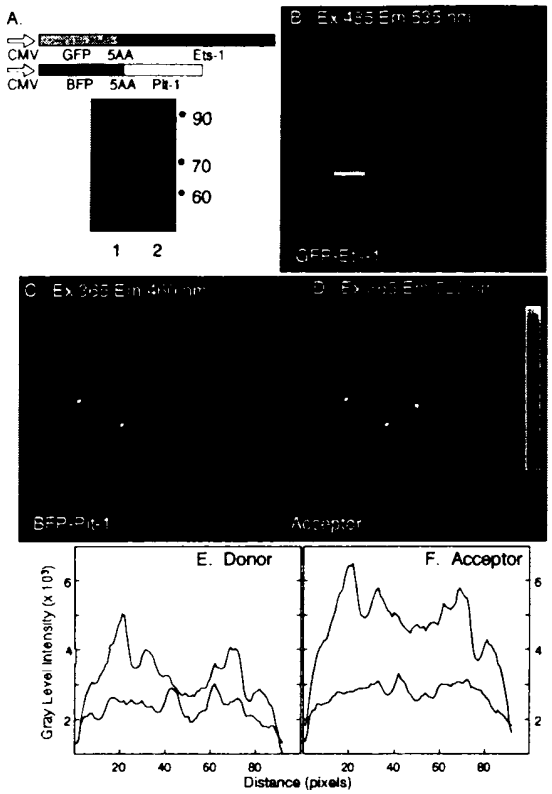

Fig. 6. FRET Microscopy of Cells Coexpressing the GFP-Ets-1 and BFP-Pit-1 Proteins

HeLa cells were transfected with vectors encoding BFP-Pit-1 or GFP-Ets-1, and expression of the proteins was detected by Western blot (panel A, lanes 1 and 2, respectively). Images of HeLa cells cotransfected with these vectors were then obtained using the GFP filter set (panel B; *bar* indicates 10 μm), BFP filter set (C), and the acceptor filter set (D). The mosaic image of donor and acceptor fluorescence (panels C and D) was acquired as described in the legend of Fig. 2. The gray level intensity profile across the two cell nuclei was taken at the position indicated in panels C and D. The *upper graph* obtained for both the donor and acceptor images (panels E and F) was from the nucleus on the *right*.

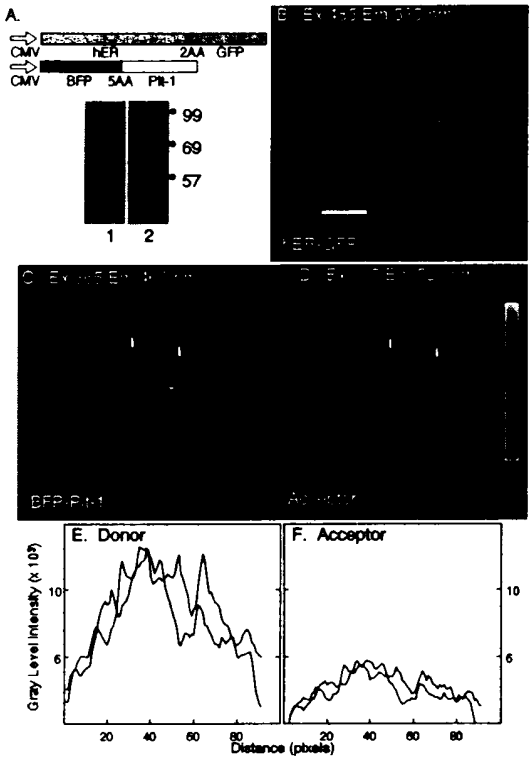

Fig. 7. FRET Microscopy of Cells Coexpressing the hER-GFP and BFP-Pit-1 Proteins

HeLa cells maintained in medium supplemented with serum containing endogenous estrogens were transfected with vectors encoding BFP-Pit-1 or hER-GFP, and expression of the proteins was detected by Western blot (panel A, lanes 1 and 2, respectively). Images of HeLa cells cotransfected with these vectors were then obtained using the GFP filter set (panel B; *bar* indicates 10 μm), BFP filter set (C), and the acceptor filter set (D). The mosaic image of donor and acceptor fluorescence (panels C and D) was acquired as described in the legend of Fig. 2. The gray level intensity profile across the two cell nuclei was taken at the position indicated in panels C and D and was then plotted for both the donor and acceptor images (panels E and F).

(data not shown). Expression of the expected 91-kDa hER-GFP fusion protein was verified by Western blotting (Fig. 7A). Cells expressing the hER-GFP protein were identified by nuclear localized green fluorescence, and coexpressed BFP-Pit-1 protein in the same cells was then confirmed by nuclear blue fluorescence (Fig. 7B). Images of cells coexpressing the two fusion proteins were acquired, and the mosaic image showing the background subtracted donor (BFP-Pit-1) and acceptor (hER-GFP) images was obtained as described above (Fig. 7, C and D). The profile of gray level intensity across the two nuclei shown in Fig. 7, E and F, demonstrated that the fluorescence signal in the acceptor image represented less than 45% of the donor signal. These results were similar to those obtained for the colocalized, but noninteracting proteins shown in Fig. 3, implying that the fluorophores labeling the estrogen receptor and Pit-1 were too far apart for FRET to occur.

DISCUSSION

The molecular cloning of GFP (25) and its expression in a variety of cell types (7, 9, 10, 26) demonstrated the potential of this unique protein as a biological marker. It is the use of GFP as fluorescent tag to visualize dynamic cellular events, however, that have proven it to be a valuable tool for the cell biologist (12, 27–29). Modifications of the GFP protein sequence have yielded variant forms with increased brightness and differing spectral characteristics (5, 6, 8). Some of the spectral variants of GFP were shown to be suitable as

donor and acceptor for FRET microscopy (8, 30). Studies by Heim and Tsien (8) determined that direct transfer of excitation energy from BFP Y66H to GFP S65T would be 50% efficient over a distance of 40 Å, and recent studies have taken advantage of FRET between these fluorophores to visualize dynamic events within the living cell. For example, FRET microscopy was used to monitor spatio-temporal changes in intracellular free calcium from single cells expressing a fusion protein containing BFP coupled to GFP by a calmodulin-binding peptide (14, 30). These studies illustrate the strength of the combined use of the GFPs and FRET microscopy to visualize the interactions of protein partners on the scale of ångstroms.

In the present study, FRET microscopy was used to visualize both homologous and heterologous protein-protein interactions involving the transcription factor Pit-1. The Pit-1 protein is a homeodomain transcription factor that is expressed exclusively in the anterior pituitary, where it functions as an important determinant of pituitary-specific gene expression (32). Pit-1 binds to DNA elements within the promoters of several different pituitary genes, including the PRL and GH genes (32–35). Biochemical studies showed that the Pit-1 protein exists as a monomer in solution, but that it binds to most DNA elements as a dimer (23, 35, 36). The Pit-1 protein contacts DNA through the carboxy-terminal POU-specific domain and homeodomain, and the dimerization contacts that form between monomers also require segments within these two domains (36). In the present study, Pit-1 proteins tagged with the GFPs were visualized in the living cell nucleus. The GFP-Pit-1 fusion protein retained both DNA binding specificity and the ability to transcriptionally activate the PRL gene promoter. When FRET microscopy was used to visualize the coexpressed BFP-Pit-1 and GFP-Pit-1 proteins, energy transfer was observed. This required that the fluorophores attached to the Pit-1 proteins be separated by less than approximately 100 Å. Due to the flexibility of Pit-1 protein structure, it is not possible to know the precise spatial positioning of the fluorophores relative to one another. This flexibility, however, might be expected to provide dynamic averaging of the relative orientations of donor and acceptor (37). Because the FRET signals obtained from cells expressing the Pit-1 proteins (Fig. 5) were similar to signals from cells expressing the GFP-three-AA-BFP fusion protein (Fig. 4), the results suggested that the GFP- and BFP-fluorophores fused to the Pit-1 proteins were in physical contact.

Since HeLa cells do not express the genes that are transcriptionally activated by Pit-1, it is unlikely that the observed FRET signals originated from dimerized Pit-1 proteins bound to specific DNA elements. It is possible that nonspecific binding of the Pit-1 fusion proteins to genomic DNA could give rise to the observed protein-protein interactions. However, there was no evidence for energy transfer from the BFP-Pit-1 protein to the hER-GFP protein (Fig. 7), demonstrating that nuclear colocalization of two DNA-binding proteins was not sufficient for FRET to occur. Further, this observation also argued against energy transfer resulting from nonspecific protein-protein interactions due to high concentrations of the donor and acceptor fusion proteins in the nuclear compartment. The actual number of fusion proteins expressed in the cells used in the present study was not determined, but it was recently shown that as few as 10,000 GFP molecules could be detected in single cells in culture (38). Since the fusion proteins used in this study were spatially localized to the nuclear compartment, still fewer GFP molecules would be required for detection. Thus, detection of GFP-fusion proteins does not require expression to levels greatly exceeding the normal physiological range for cellular proteins, and nonspecific interactions between fusion proteins was an unlikely source of energy transfer signals.

It is clear that binding to specific DNA elements leads to dimerization of Pit-1 proteins (36). It was therefore somewhat surprising that FRET imaging should reveal Pit-1 protein-protein interactions in the absence of specific DNA contacts in the HeLa cell nucleus. It is possible that the Pit-1 fusion proteins are assembling as part of larger complexes of nuclear proteins, and a number of transcription factors have been shown to cooperatively interact with Pit-1. In transfection studies in nonpituitary cells, cooperative interactions between Pit-1 and other non-cell type-specific transcription factors was shown to be required for transcriptional activation of the PRL promoter. These studies lead to the demonstration of a strong synergy between Pit-1 and members of the *ets* transcription factor family (18, 19), and biochemical studies showed that Pit-1 and Ets-1 could physically associate (20). In the present study, the results of FRET imaging of Pit-1 and Ets-1 proteins provided evidence for energy transfer between the fluorophores (Fig. 6), indicating that these proteins were in physical contact or close association in the cell nucleus. The relatively weak FRET signals obtained with Pit-1 and Ets-1 may indicate that the fluorophores were separated by a distance close to the limit necessary for energy transfer.

Previous studies also demonstrated that cooperative interactions involving Pit-1 and the estrogen receptor were important in regulation of the PRL gene transcription (21–24). As was the case for Ets-1, biochemical studies demonstrated that physical interactions also occurred between Pit-1 and the estrogen receptor (24). In contrast to the results obtained with Ets-1 and Pit-1 in the present study, FRET imaging provided no evidence for energy transfer between the fluorophores attached to Pit-1 and the estrogen receptor (Fig. 7). Given the extremely restricted distance over which FRET can occur, it is conceivable that Pit-1 and estrogen receptor proteins were in physical contact, but that the fluorophores were separated by more than 100 Å or obstructed in some way. It was recently shown that the coactivator protein RIP140 participates in the molecular interactions between Pit-1 and the

estrogen receptor (39), and this protein could potentially act as a spacer between the fusion proteins.

The results from this experiment also illustrated an important limitation of the FRET techninque; while positive results demonstrate physical interactions between protein partners, a negative result provides no information about protein-protein interactions. The results presented here demonstrated that Pit-1 proteins were in physical contact in these living HeLa cell nuclei, and also implicated that Pit-1 and Ets-1 were in close association. It is possible that these proteins come in contact as part of complexes involving other nuclear proteins. In support of this view, we reported previously the use of a digital deconvolution computer algorithm to process images of GFP-Pit-1 acquired at different optical sections through the cell nucleus (40). The resulting high-resolution images demonstrated an ordered pattern of Pit-1 localization within the nuclear compartment that may indicate inclusion of the fusion proteins within subnuclear structures (41). Taken together, the results presented here illustrate the utility of FRET microscopy to visualize interactions between protein partners tagged with the GFPs in the living cell.

MATERIALS AND METHODS

Materials

Construction of some of the GFP- and BFP-fusion protein expression vector DNAs was described previously (15, 16). The sequences encoding GFP (S65T; Ref. 6), and BFP (Y66H, Y145F; Ref. 5) were modified for optimal mammalian cell expression through human codon usage (15, 42). A plasmid vector using the strong cytomegalovirus promoter (pCMV) was used for expression of all the fluorescent fusion proteins (43). The sequence encoding Pit-1(29) and cEts-1 (44) were obtained by PCR amplification with the proofreading KlenTaq polymerase mix (CLONTECH Laboratories, Inc., Palo Alto, CA) using the cloned DNA sequences as templates. Introduction of unique restriction endonuclease sites into the amplified DNA facilitated in-reading frame insertion of these sequences at the extreme 3′-end of the coding sequence for GFP and BFP. The sequence encoding the human estrogen receptor AA 1–576 linked to GFP(S65T) was resected from the pNEFGFPS65T vector (kindly provided by Dr. D. Picard, Universite de Geneve, Geneva, Switzerland) and inserted into the pCMV vector. The pCMV GFP-three-AA-BFP vector encoding GFP fused to BFP by a three-AA linker was prepared by ligation of the BFP cDNA into the GFP vector, placing the BFP coding sequence in the reading frame of GFP. The vector encoding GFP with NLS was prepared by insertion of a duplex oligonucleotide sequence encoding the SV40 NLS (45) protein sequence LYPKKKRKGVEDQYK at the 3′-terminus of the GFP coding sequence. For transfection, large-scale recovery of expression vector plasmid DNAs was performed by double-banded CsCl gradient centrifugation, and the plasmid DNAs were verified by restriction enzyme analysis and direct sequence analysis.

Cell Culture and Transfection

HeLa cells or Rat 1 cells were maintained as a monolayer in a 1:1 mixture of phenol red-free Ham's F12-DMEM containing 10% newborn calf serum. The cells were harvested and transfected with the indicated genetic vector(s) by electroporation as described previously (46). For the luciferase reporter gene experiments, the total amount of DNA was kept constant using empty vector DNA. After electroporation, the cells were immediately diluted in medium and used to inoculate culture dishes for analysis of luciferase reporter gene activity, or for preparation of cell extracts for Western blot analysis or EMSA. Luciferase assays were performed as described previously (46). For imaging of GFP- and BFP-fusion protein expression, transfected cells were used to inoculate culture dishes containing 25-mm glass cover slips. These cultures were maintained at 33 C in a humidified 5% CO_2 incubator for 24 h before fluorescence microscopy for optimized protein expression (38).

Western Blotting and EMSA

Transiently transfected HeLa cells were lysed at 4 C in detergent buffer as described previously (46). Samples were fractionated by SDS-PAGE on 10% gels. Protein standards were run in adjacent lanes for determination of mol wt. The proteins were transferred to nitrocellulose for 1 h by electroblotting at 100 V and then detected by Ponceau S staining. The membranes were blocked with 5% nonfat dried milk in TBS-T buffer [20 mM Tris-HCl (pH 7.6), 137 mM NaCl, 0.1% Tween-20], washed in TBS-T, and incubated with GFP antibody (Molecular Probes, Eugene, OR; 1:10,000 final dilution) for 1 h at room temperature. After washes in TBS-T, the membranes were incubated with a 1:50,000 final dilution of horseradish peroxidase-conjugated antirabbit Ig (Amersham Corp., Arlington Heights, IL). The membranes were washed in TBS-T and incubated in enhanced chemiluminescence (ECL) reagents (DuPont/NEN, Boston, MA) for 1 min. The membranes were then exposed to Kodak XAR 5 film (Eastman Kodak, Rochester, NY) for 5–15 min.

EMSAs were performed on whole cell extracts prepared from transiently transfected HeLa cells as described previously (46). A duplex oligonucleotide corresponding to the 3P-PRL Pit-1 binding site (5′-GGAGGCCTGAATATGAA-TAAGA, Ref. 19) was end labeled using [γ-^{32}P] ATP and T4 polynucleotide kinase and used as probe. Whole cell extract (20 μg) was added to 15 μl reaction mixtures assembled on ice. For immunoclearing experiments, 0.75 μl Pit-1 polyclonal antibody was added to the reaction mixtures and incubated for 1 h at 4 C. The reaction mixtures were transferred to tubes containing 25,000 to 50,000 cpm of the end labeled probe. The mixtures were then incubated for 20 min at room temperature and loaded on prerun 6.0% polyacrylamide gels prepared in running buffer containing 25 mM Tris-HCl (pH 8.3), 192 mM glycine, 1 mM EDTA. The gels were run at 150 V, dried, and autoradiographed overnight using Kodak XAR 5 film.

Fluorescence Microscopy

The FRET imaging system used in these studies is based on a conventional inverted microscope equipped for epi-fluorescence and transmitted illumination (IX-70, Universal infinity system; Olympus America, Inc., Melville, NY). Fluorescence images were acquired using a 60× aqueous-immersion objective lens. The excitation light source was a 100 W mercury-xenon arc lamp (Hamamatsu Corp., Middlesex, NY) coupled to excitation and nd filter wheels. The emission filter wheel was coupled to the output port of the microsocope and then to the camera. Images were captured using a slow scan, liquid nitrogen-cooled charge-coupled device camera with a back-thinned, back-illuminated imaging chip (CH260, Photometrics, Ltd., Tucson, AZ). The digital image output of the camera was 512 × 512 pixels with 16 bits resolution. For these studies, all images were collected using a nd 1.0 filter and constant integration times. All fluorescence signals fell within the range of 10 to 35 K gray level intensity (before

background subtraction), and none of the images had saturated pixels. The Silicon Graphics, Inc.-based ISEE software (Inovision Corporation, Raleigh, NC) was then used to obtain the mosaic images and determine the gray level intensity profiles.

Acknowledgments

The author is grateful to Dr. Ammasi Periasamy of the Advanced Cellular Imaging Facility at the University of Virginia for expert assistance in imaging and the technical assistance of Diana Berry and Margaret Kawecki. The author also wishes to thank Dr. David Brautigan for helpful discussion and comments. The mutant GFP S65T and Y66H/Y145F cDNAs were provided by Drs. Roger Tsien and Roger Heim (University of California, San Diego, CA), and Dr. Jen Sheen (Massachusetts General Hospital, Boston, MA) provided the mutant GFP with optimized codon usage.

Received April 7, 1998. Revision received April 30, 1998. Accepted May 27, 1998.

Address requests for reprints to: Richard N. Day, Ph.D., Department of Internal Medicine, Box 578, University of Virginia Health Sciences Center, Charlottesville, Virginia 22903. E-mail: rnd2v@virginia.edu.

This study was supported by National Science Foundation (NSF) Grant DIR-8920162, Center for Biological Timing Technology Development subproject, and NSF Grant IBN9528526 and NIH Grant RO1-DK-43701.

REFERENCES

1. Stryer L 1978 Fluorescence energy transfer as a spectroscopic ruler. Annu Rev Biochem 47:819–846
2. Cheung HC 1991 Resonance energy transfer. In: Lakowicz JR (ed) Topics in Fluorescence Spectroscopy, Principles. Plenum Press, New York, vol 2:127–176
3. Wu P, Brand L 1994 Resonance energy transfer: methods and applications. Anal Biochem 218:1–13
4. Förster T 1967 Mechanism of energy transfer. In: Florkin M., Statz EH (eds) Comprehensive Biochemistry. Elsevier, New York, pp 61–77
5. Heim R, Prasher DC, Tsien RY 1994 Wavelength mutations and posttranslational autoxidation of green fluorescent protein. Proc Natl Acad Sci U S A 91:12501–12504
6. Cubitt AB, Heim R, Adams SR, Boyd AE, Gross LA, Tsien RY 1995 Understanding, improving and using green fluorescent proteins. Trends Biochem Sci 20:448–455
7. Plautz JD, Day RN, Dailey GM, Welsh SB, Hall JC, Halpain S, Kay SA 1996 Green fluorescent protein and its derivatives as versatile markers for gene expression in living *Drosophila melanogaster*, plant and mammalian cells. Gene 173:83–87
8. Heim R, Tsien RY 1995 Engineering green fluorescent protein for improved brightness, longer wavelengths and fluorescence resonance energy transfer. Curr Biol 6:178–182
9. Rizzuto R, Brini M, De Giorgi F, Rossi R, Heim R, Tsien RY, Pozzan T 1996 Double labeling of subcellular structures with organelle-targeted GFP mutants *in vivo*. Curr Biol 6:183–188
10. Gerdes HH, Kaether C 1996 Green fluorescent protein: applications in cell biology. FEBS Lett 389:44–47
11. Ludin B, Doll T, Meili R, Kaech S, Matus A 1996 Application of novel vectors for GFP-tagging of proteins to study microtubule-associated proteins. Gene 173:107–111
12. Carey KL, Richards SA, Lounsbury KM, Macara IG 1996 Evidence using a green fluorescent protein-glucocorticoid receptor chimera that the Ran/TC4 GTPase mediates an essential function independent of nuclear protein import. J Cell Biol 133:985–996
13. Mitra RD, Silva CM, Youvan DC 1996 Fluorescence resonance energy transfer between blue-emitting and red-shifted excitation derivatives of the green fluorescent protein. Gene 173:13–17
14. Romoser VA, Hinkle PM, Persechini A 1997 Detection in living cells of Ca2+-dependent changes in the fluorescence emission of an indication composed of two green fluorescent protein variants linked by a calmodulin-binding sequence: a new class of fluorescent indicators. J Biol Chem 272:13270–13274
15. Periasamy A, Kay SA, Day RN 1997 Fluorescence resonance energy transfer (FRET) imaging of a single living cell using green fluorescent protein. SPIE Proc: Functional Imaging and Optical Manipulation of Living Cells 2983:58–66
16. Periasamy A, Day RN 1998 Digitized GFP imaging and FRET microscopy. In: Kay SA, Sullivan KF (eds) Methods in Cell Biology. American Society of Cell Biology, Academic Press, San Diego, CA, in press
17. Periasamy A, Day RN 1998 FRET imaging of Pit-1 protein interactions in living cells. J Biomed Optics 3:154–160
18. Bradford AP, Conrad KE, Wasylyk C, Wasylyk B, Gutierrez-Hartmann A 1995 Functional interaction of c-Ets-1 and GHF-1/Pit-1 mediates Ras activation of pituitary-specific gene expression: mapping of the essential c-Ets-1 domain. Mol Cell Biol 15:2849–2857
19. Howard PW, Maurer RA 1995 A composite Ets/Pit-1 binding site in the prolactin gene can mediate transcriptional responses to multiple signal transduction pathways. J Biol Chem 270:20930–20936
20. Bradford AP, Wasylyk C, Wasylyk B, Gutierrez-Hartmann A 1997 Interaction of Ets-1 and the POU-Homeodomain protein GHF-1/Pit-1 reconstitutes pituitary specific gene expression. Mol Cell Biol 17:1065–1074
21. Day RN, Koike S, Sakai M, Muramatsu M, Maurer RA (1990) Both Pit- 1 and the estrogen receptor are required for estrogen responsiveness of the rat PRL gene. Mol Endocrinol 4:1964–1971
22. Simmons DM, Voss JW, Ingraham HA, Holloway JM, Broide RS, Rosenfeld MG, Swanson LW 1990 Pituitary cell phenotypes involve cell-specific Pit-1 mRNA translation and synergistic interactions with other classes of transcription factors. Genes Dev 4:696–711
23. Holloway JM, Szeto DP, Scully KM, Glass CK, Rosenfeld MG (1995) Pit- 1 binding to specific DNA sites as a monomer or dimer determines gene-specific use of a tyrosine-dependent synergy domain. Genes Dev 9:1992–2006
24. Nowakowski BE, Maurer RA (1994) Multiple Pit-1-binding sites facilitate estrogen responsiveness of the prolactin gene. Mol Endocrinol 8:1742–1749
25. Prasher DC, Eckenrode VK, Ward WW, Prendergast FG, Cormier MJ 1992 Primary structure of the *Aequorea victoria* green-fluorescent protein. Gene 111:229–233
26. Chalfie M, Tu Y, Euskirchen G, Ward WW, Prasher DC 1994 Green fluorescent protein as a marker for gene expression. Science 263:802–805
27. Presley JF, Cole NB, Schroer TA, Hirschberg K, Zaal KJ, Lippincott-Schwartz J 1997 ER-to-Golgi transport visualized in living cells. Nature 389:81–85
28. Lee MS, Henry M, Silver PA 1996 A protein that shuttles between the nucleus and the cytoplasm is an important mediator of RNA export. Genes Dev 10:1233–1246
29. Wacker I, Kaether C, Kromer A, Migala A, Almers W, Gerdes HH 1997 Microtubule-dependent transport of secretory vesicles visualized in real time with a GFP-tagged secretory protein. J Cell Sci 110:1453–1463
30. Miyawaki A, Llopis J, Heim R, McCaffery JM, Adams JA,

Ikura M, Tsien RY (1997) Fluorescent indicators for Ca2+ based on green fluorescent proteins and calmodulin. Nature 388:882–887
32. Andersen, B, Rosenfeld, MG 1994 Pit-1 determines cell types during development of the anterior pituitary gland. A model for transcriptional regulation of cell phenotypes in mammalian organogenesis. J Biol Chem 269:29335–29338
33. Ingraham HA, Chen R, Mangalam HJ, Elsholtz HP Flynn SE, Lin CR, Simmons DM, Swanson LW, Rosenfeld MG 1988 A tissue-specific transcription factor containing a homeodomain specifies a pituitary phenotype. Cell 55:519–529
34. Theill LE, Castrillo JL, Wu D, Karin M 1989 Dissection of functional domains of the pituitary-specific transcription factor GHF-1. Nature 342:945–948
35. Ingraham, HA, Flynn, SE, Voss, JW, Albert, VR, Kapiloff, MS, Wilson, Rosenfeld, MG 1990 The POU-specific domain of Pit-1 is essential for sequence specific, high affinity DNA binding and DNA dependent Pit-1-Pit-1 interactions. Cell 61:519–529
36. Jacobson EM, Peng L, Leon-del-Rio A, Rosenfeld MG, Aggarwal AK 1997 Structure of Pit-1 POU domain bound to DNA as a dimer: unexpected arrangement and flexibility. Genes Dev 11:198–212
37. dos Remedios CG, Moens PDJ 1995 Fluorescence resonance energy transfer spectroscopy is a reliable "ruler" for measuring structural changes in proteins. Dispelling the problem of the unknown orientation factor. J Struct Biol 115:175–185
38. Patterson GH, Knobel SM, Sharif WD, Kain SR, Piston DW 1997 Use of the green fluorescent protein and its mutants in quantitative fluorescence microscopy. Biophys J 73:2782–2790
39. Chuang FM, West BL, Baxter JD, Schaufele F 1997 Activities in Pit-1 determine whether receptor interacting protein 140 activates or inhibits Pit-1/nuclear receptor transcriptional synergy. Mol Endocrinol 11:1332–1341
40. Periasamy A, Day RN 1997 Pit-1 protein localization at different optical sections in a single living cell using FRET microscopy and green fluorescent proteins. In: Bailey GW, Dimlich RVW, Alexander KB, McCarthy JJ, Pretlow TP (eds) Proceedings of Microscopy and Microanalysis. Springer-Verlag, New York, vol 3:133–134
41. Spector DL 1993 Macromolecular domains within the cell nucleus. Annu Rev Cell Biol 9:265–315
42. Chiu W, Niwa Y, Zeng W, Hirano T, Kobayashi H, Sheen J 1996 Engineered GFP as a vital reporter in plants. Curr Biol 6:325–330
43. MacGregor GR, Caskey CT 1989 Construction of plasmids that express *E. coli* beta-galactosidase in mammalian cells. Nucleic Acids Res 17:2365
44. Kalderon D, Roberts BL, Richardson WD, Smith AE 1984 A short amino acid sequence able to specify nuclear location. Cell 39:499–509
45. Mavrothalassitis G, Fisher RJ, Smyth F, Watson DK, Papas TS 1994 Structural inferences of the ETS1 DNA-binding domain determined by mutational analysis. Oncogene 9:425–435
46. Day RN, Day KH 1994 Specific repression of rat prolactin gene expression in transplanted tumor cells. Mol Endocrinol 8:12–20